Available online at www.sciencedirect.com
ScienceDirect
Journal of the European Ceramic Society 30 (2010) 1919–1924
www.elsevier.com/locate/jeurceramsoc

Grain size effect on electromechanical properties and non-linear response of dense nano and microstructured PIN–PT ceramics

K. Alilat [a,b], M. Pham Thi [a], H. Dammak [b,*], C. Bogicevic [b], A. Albareda [c], M. Doisy [d]

[a] *Laboratoire Nanocomposites & Matériaux Multifonctionnels, Thales Research & Technology-France, RD 128, F-91767 Palaiseau Cedex, France*
[b] *Laboratoire Structures, Propriétés et Modélisation des Solides UMR 8580 CNRS, Ecole Centrale de Paris, Grande voie des vignes, 92295 Châtenay-Malabry, France*
[c] *Department of Applied Physics, Universitat Politecnica de Catalunya, Jordi Girona 1-3, modul B4, 08034 Barcelona, Spain*
[d] *Thales Underwater Systems, Route des Dolines, 525 Route des Dolines, BP157, 06905 Sophia Antipolis, France*

Received 13 October 2009; received in revised form 18 February 2010; accepted 17 March 2010

Abstract

Nanopowders of $0.63Pb(In_{1/2}Nb_{1/2})O_3$–$0.37PbTiO_3$ were synthesized by solid state reaction using the continuous attrition milling followed by high-energy ball milling techniques in air at room temperature. After milling for 8 h nanopowders of 20–30 nm grain size are obtained. Sintering by hot pressing of PIN–37PT green pellets leads to dense ceramics with average grain size varying from 100 nm to 1 μm. The dielectric and piezoelectric properties of PIN–37PT nanostructured ceramics with grain size bigger than about 160 nm remain roughly unchanged and comparable to those of microstructured ceramics. In addition, the stability of the permittivity and dielectric losses under high ac electric field grows when the grain size decreases. The material becomes less non-linear with decreasing grain size. This result is attractive for acoustic transducer applications.

Keywords: A. Hot pressing; B. Grain size; C. Piezoelectric properties; D. Perovskites

1. Introduction

Lead indium niobium ceramics $(1-x)Pb(In_{1/2}Nb_{1/2})$–$xPbTiO_3$ (PIN–PT) present a high Curie temperature and exhibit excellent dielectric and electromechanical properties at low and high signal, especially at compositions near the morphotropic phase boundary (MPB).[1] It is important to note that the higher the Curie temperature, the higher the coercive field, and the required electric field. This system, not extensively studied, represents a great interest for piezoelectric actuators, underwater and medical acoustic transducers.

Previous work on PIN–PT microstructured ceramics near the MPB ($x=0.37$) had revealed a high Curie temperature $T_C \sim 300\,^{\circ}C$,[1,2] high dielectric and piezoelectric properties (ε_{33}^{T} at 1 kHz = 2600, $k_p \sim 0.57$), a high coercive field ($E_c = 1600$ V/mm) and had observed a relatively good stability of dielectric constant under high ac field.[3] The X-ray diffraction and dielectric studies have shown that the MPB zone of PIN–PT system separates a rhombohedral phase for low PT compositions from a tetragonal phase for high PT compositions. The composition near the MPB, PIN–37PT ($x=0.37$) presents a phase transition from a monoclinic phase to a tetragonal phase at $T_{F-F} \sim 150\,^{\circ}C$.[4] Since PIN–PT ceramics are attractive for high-power sonar application, it is important to know if the ceramics with nano-size grains can improve the properties at high signal. However, the difficulty in preparing nanostructured ceramic materials includes not only the synthesis of nanopowders but also their consolidation, shaping, and subsequent sintering. The sintering by hot forging of nanostructured ceramics represents a compromise between pressure and temperature. The goal of this work is to show the influence of the grain size on structure, electromechanical properties and non-linear dielectric properties of nanostructured ceramics under high ac field. We compare these properties with those of conventional PIN–PT and of hard PZT[5] microstructured ceramics.

2. Experimental procedure

PIN–xPT ceramics were synthesized by a two-step solid state reaction via Wolframite. The Wolframite ($InNbO_4$) was formed

* Corresponding author. Tel.: +33 1 41131580; fax: +33 1 41131437.
E-mail address: hichem.dammak@ecp.fr (H. Dammak).

0955-2219/$ – see front matter © 2010 Elsevier Ltd. All rights reserved.
doi:10.1016/j.jeurceramsoc.2010.03.010

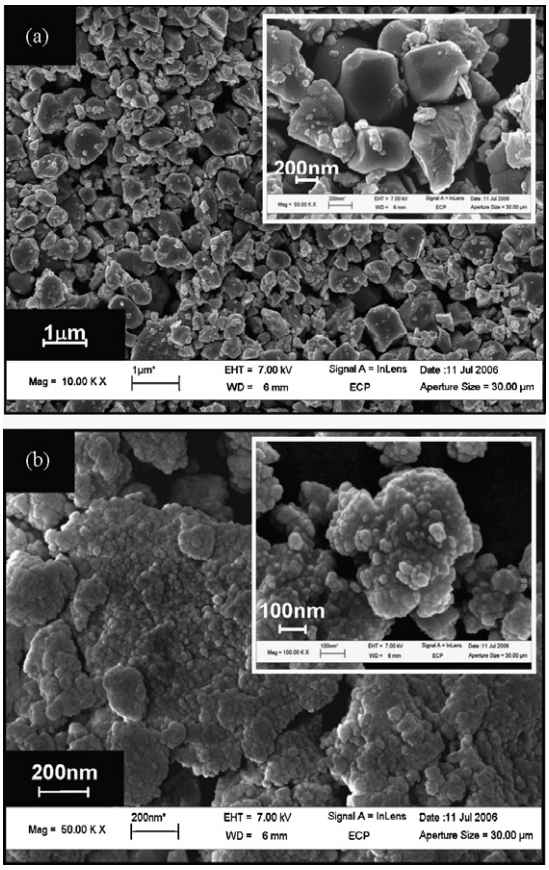

Fig. 1. SEM micrograph of PIN–PT perovskite micropowder obtained by attrition milling (a) and nanopowder obtained by high-energy milling (b).

by mixing In_2O_3 with Nb_2O_5 at 1100 °C for 24 h and then mixed with PbO and TiO_2. The mixture was ball-milled, dried and calcined at 850 °C for 2 h to form stoichiometric perovskites. The ultra fine perovskite powder (Fig. 1a), exhibiting high specific areas, S_{BET} = 12 m^2/g, consists of a major grains of about 0.4 μm and nanoparticles upon their surface; it was obtained by continuous attrition milling. Then, a specially equipped Retsch mill PM400 was used for high-energy ball milling during 8–10 h. The high-energy-milled powder consists of agglomerates constituted by crystalline nanograin sizes (primary particle sizes of ~20 nm, Fig. 1b). The energy dispersive X-ray analysis of powders shows that contamination by Zr from ZrO_2 milling media was below 300 ppm.

Nanopowders were first uniaxially pressed at 300 MPa and green ceramics pellets with density of about 50–60% were obtained. The green PIN–PT pellets were embedded in Al_2O_3 powder and then sintered by hot pressing at temperatures ranging between 750 °C and 1200 °C for 1 h under pressures ranging between 0 MPa and 500 MPa. Different PIN–PT ceramics with high relative densities (>98% of the theoretical density) and different grain size were prepared.

High resolution X-ray diffraction (XRD) measurements were performed on a highly accurate two-axis diffractometer in a Bragg-Brentano geometry with Cu-K_β wavelength issued from an 18 kW Rigaku rotating anode generator, using a furnace operating between RT and 400 °C. Structural refinement was carried out on these XRD patterns at 350 °C and 200 °C with the XND program[6] in order to determine the lattice parameters of the cubic and tetragonal phases.

The average grain size of nanopowders and nanostructured ceramics was measured, using the line intersection method, on scanning electron microscope (SEM) images obtained at room temperature and compared to the average grain size obtained by refinement of XRD patterns recorded for the cubic phase at 350 °C. The attrition milled and high-energy-milled powders consist of pure perovskite phase, without the presence of amorphous phase or pyrochlore phases. XRD refinement results in a size of about 20–22 nm which is coherent with SEM observations.

For electric measurements, silver paint was deposited on the polished faces and fired at 500 °C during 30 min. Ceramics were poled by field cooling process. Dc electric fields, 2.5–3 kV/mm, were applied to samples in silicon oil at 170 °C and then cooled down to 40 °C. Temperature dependence of the dielectric constant was measured at 1 kHz using a HP 4192A impedance analyzer. Electromechanical properties were measured according to the IRE standard method with an Agilent 4294A impedance analyser. Drift measurements or electric field dependences of the dielectric constant and dielectric losses were measured up to 1 kV/mm. The sinusoidal signal at 1 kHz, generated from a HP 3314A function generator, was amplified by a Kepco Bipolar Amplifier. A EG&G 5210 Lock-in Amplifier and an integration capacitance allow to measure the capacitance and the dielectric losses (tan δ) at fundamental frequency.

3. Results and discussion

3.1. Phase transitions and ferroelectric distortion

Ceramics obtained from attrition milled powder, by using the conventional sintering at ambient pressure and at 1200 °C, exhibit homogeneous microstructure with a 1–2 μm grain size. Fig. 2 shows the SEM micrographs of PIN–37PT dense ceramics sintered from nanopowder by hot forging at different pressures. Ceramics present homogeneous microstructures with a grain size of about 250–300 nm, 125–180 nm and 50–125 nm (Fig. 2a–c), respectively. For easier presentation, we annotate these ceramics by using their average grain size: 1 μm, 300 nm, 160 nm and 100 nm, respectively.

Fig. 3 shows the pseudo-cubic (2 0 0) X-ray diffraction peak of PIN–37PT microstructured and nanostructured ceramics for different temperatures. As expected, the pattern at 350 °C ($>T_C$) shows single peaks characteristic of the cubic phase (Fig. 3a). When decreasing the temperature to 200 °C, the (2 0 0) reflection of the microstructured ceramic becomes asymmetric due to the diffuse shoulder on its left side, attributed to the transition into a tetragonal phase. The (2 0 0) reflection of the nanostructured ceramic remains symmetric (Fig. 3b), but the small broadening shows that its tetragonal distortion is lower than that of the microstructured one. At room temperature, the (2 0 0) reflection of PIN–37PT microstructured ceramic is broader and more diffuse than the (2 0 0) reflection of PIN–37PT nanostructured ceramic (Fig. 3c). It was shown that a mixture of a tetrago-

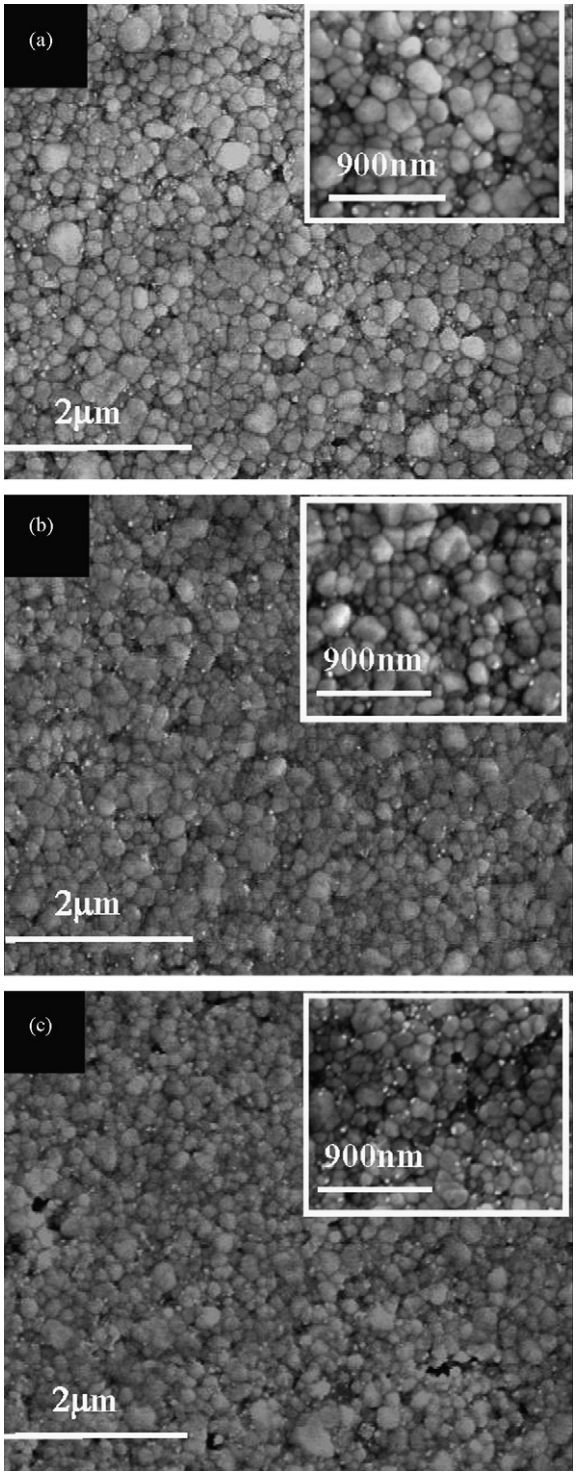

Fig. 2. SEM micrograph showing the microstructures of PIN–PT ceramic sintered by hot forging: 900 °C, 300 MPa (a), 850 °C, 400 MPa (b) and 750 °C, 500 MPa (c).

nal phase and monoclinic or rhombohedral phase are obtained at room temperature[4]: a mixture of these two phases would be responsible for diffuse shoulders. In order to observe the phase transition and ferroelectric distortion, the full width at half maximum (FWHM) was determined by a fit using one asymmetric peak. Fig. 3d shows the ceramic grain size dependence

Table 1
Dielectric and electromechanical properties of PIN–37PT ceramics exhibiting the grain size of 1 μm, 300 nm, 160 nm and 100 nm.

ρ (% ρ_{th})	PIN–37PT				PZT-4D
	98	98.4	98	98	99
Grains size	1 μm	300 nm	160 nm	100 nm	5 μm
$\varepsilon_{33}^{T}/\varepsilon_0$ at 1 kHz	2286	2210	2155	2016	1300
$\tan(\delta_e)$ at 1 kHz	0.02	0.019	0.018	0.018	0.004
d_{33} (pC/N)	450	430	420	315	315
k_p	0.55	0.52	0.51	0.44	0.57
Q_m	70	76	85	78	600
m_ε	0.44	0.38	0.41	0.42	0.19
α ($\times 10^{-3}$ m/V)	2.1	1.25	0.54	0.49	0.49

The ratio m_ε and the Rayleigh coefficient α are determined from high ac field measurements. Values for PZT-4D were measured in the same conditions and are given for comparison.

of the (2 0 0) FWHM. At 350 °C, i.e. in the cubic phase, the FWHM follows the grain size: it increases when the grain size decreases. For all ceramics, the FWHM increases with decreasing temperature. This is consistent with the transition from paraelectric cubic phase to ferroelectric phases. For any temperature, lower than T_C, the increase of the FWHM with increasing grain size corresponds to an increase of a ferroelectric distortion or/and to a mixture of two phases.[7] In addition, the tetragonal lattice parameters extracted by refinement at 200 °C yield a *c*/*a* ratio of 1.0044, 1.0037 and 1.0036 for 1 μm, 300 nm and 160 nm nanostructured ceramics, respectively. This indicates, decreasing ferroelectric distortion of nanostructured ceramics with decreasing grain size. For 100 nm grain sized ceramics, we have observed an unexpected behaviour: an important reduction of the lattice parameters (Fig. 4). This result suggests that, below a critical size, other mechanisms are taking place. In fact, in the case of $(PbMg_{1/3}Nb_{2/3}O_3)0.8$–$(PbTiO_3)0.2$ (PMN–PT)[8] a phase transition from a monoclinic phase to a rhombohedral one is observed, around a critical grain size ~200 nm, when the grain size decreases. This effect, called grain size-induced polarization rotation, should also exist in our case.

3.2. Dielectric constant versus temperature and electromechanical properties

Table 1 resumes the electromechanical constants for four average grain sizes of PIN–37PT dense ceramics and shows, as a comparison, the values for PZT-4D. One notes that PIN–37PT presents piezoelectric properties approaching those of PZT-4D. Like the dielectric constant, the piezoelectric constant and the planar coupling factor decrease only little when the grain size decreases down to 160 nm. However, the electromechanical constants obtained on 100 nm nanostructured ceramic were much lower than those of the 160 nm nanostructured ceramic. This is could be due to a reduction of ferroelectricity and spontaneous polarization when the grain size is smaller than 160 nm as observed in $BaTiO_3$.[9] As it will be explained later, the reduction of extrinsic effects caused by the decrease of the grain size could explain the decrease of these coefficients.

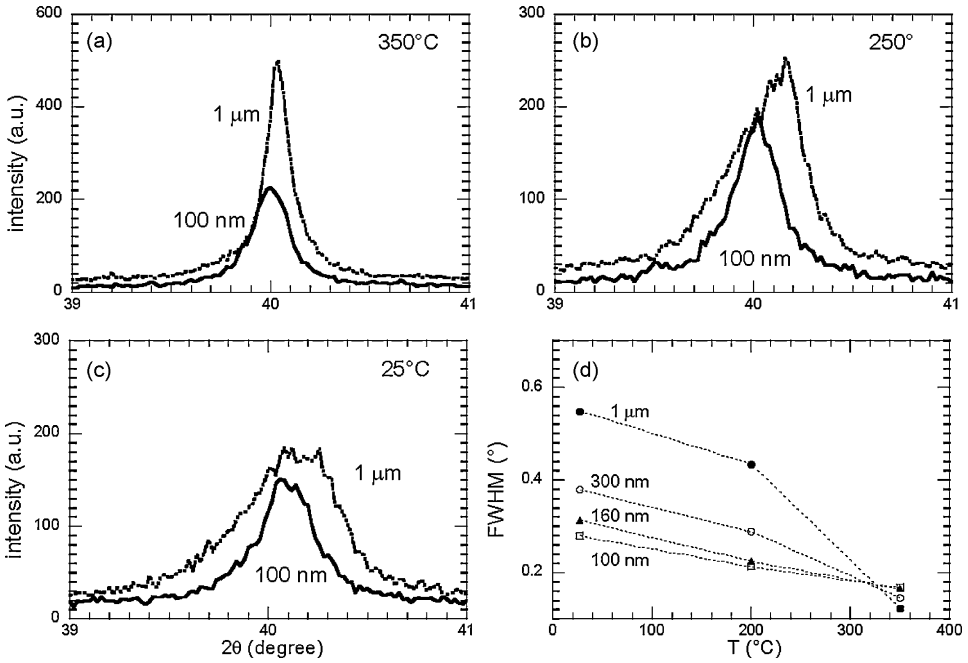

Fig. 3. XRD pattern showing the evolution of the (2 0 0) peak of PIN–37PT micro and nanostructured ceramics at 350 °C (a), 200 °C (b) and 25 °C (c); and the thermal evolution of the full width at half maximum of the (2 0 0) peak (d).

Concerning PIN–37PT nanostructured ceramics, Fig. 5a shows the temperature dependence of the dielectric constant ($\varepsilon_{33}^{T}/\varepsilon_0$) of PIN–PT poled ceramics with different grain sizes during a zero-field heating process. The two large anomalies in the dielectric curves near 150 °C and 320 °C are consistent with the ferroelectric–ferroelectric transition and the well known tetragonal–cubic phase transition. At RT the dielectric constant of ceramics remains roughly unchanged ($\varepsilon_{33}^{T}/\varepsilon_0 \cong 2200$) for 1 μm, 300 nm and 160 nm grain sized ceramics whereas it decreases for the 100 nm grain size ($\varepsilon_{33}^{T}/\varepsilon_0 \cong 1900$) (Fig. 5b). The dielectric curves become more and more diffuse and ε_{max} drops rapidly for 300 nm and 160 nm grain sized ceramics (Fig. 5c). On the other hand, the temperature of the dielectric constant maximum, T_{max}, remains roughly constant when the grain size decreases.

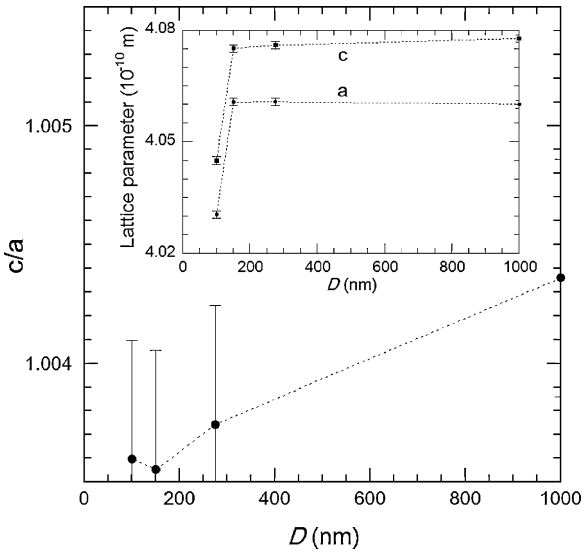

Fig. 4. Tetragonal distortion of PIN–PT ceramics at 200 °C with decreasing grain size. The inset shows the lattice parameters evolution.

3.3. Drift of the dielectric properties

In sonar applications, the driven electric field is up to 400 V/mm, is much higher than in the IRE standard measurements (<1 V/mm). In such conditions, piezoelectric ceramics display a remarkable non-linear behaviour. The linear increase in dielectric constant with the applied field is often consistent with the linear increase of the reverse piezoelectric coefficient. The same behaviour is observed for dielectric loss. However, the dielectric and piezoelectric coefficients are quite different in a high-power device from that with a low signal. There are two effects concerning dielectric and piezoelectric responses. The reversible intrinsic effect, due to the elastic deformation, depends mainly on the proportion and orientation of the different ferroelectric domains while the extrinsic effect, due to wall domain motion or the rotation of dipoles, is caused by the presence of defects. Both contributions depend on the crystal structure. Ceramic microstructure affects both intrinsic and extrinsic contributions and the non-linear behaviour is usually related exclusively to extrinsic mechanisms. The increase of the dielectric constant is related to the extrinsic contribution corresponding to the wall domain motion under high electric field.[10,11] The reduction of dielectric constant, shown in the previous paragraph, implies that the extrinsic effect is lower when the grain size decreases, so it is expected that the non-linear contribution will be lower as well. The ac electric field dependence of the dielectric constant $\varepsilon_{33}^{T}/\varepsilon_0$ and dielectric losses tan δ_e at 1 kHz for poled ceramics are drawn in Fig. 6. These figures show clearly that the smaller the grain size of PIN–37PT nanos-

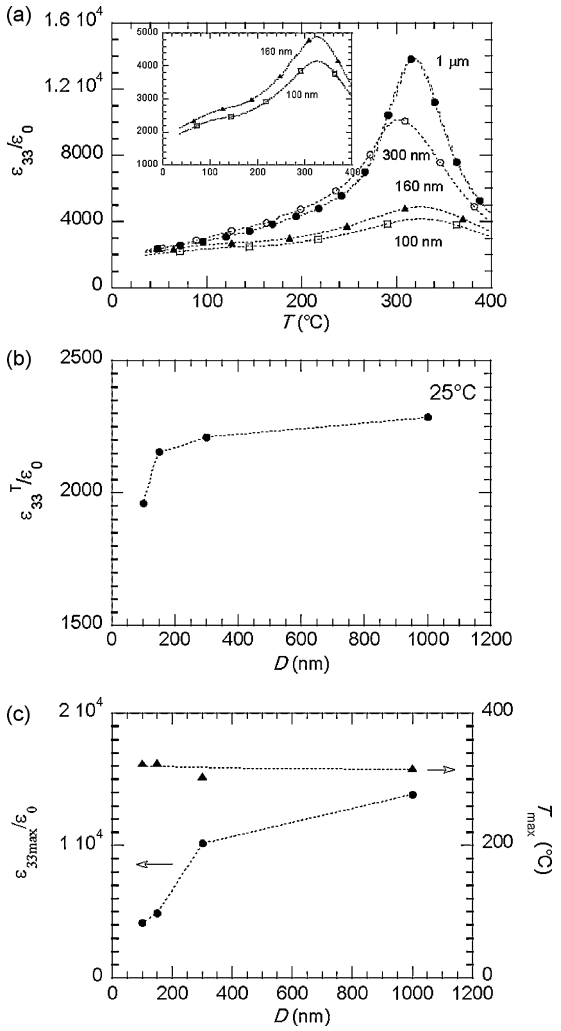

Fig. 5. Temperature dependence of the dielectric constant ε_{33}^{T} at 1 kHz for different grain sizes of poled PIN–37PT micro and nanostructured ceramics (a); grain sizes dependence of $\varepsilon_{33}^{T}/\varepsilon_0$ at RT (b), ε_{max} and T_{max} (c).

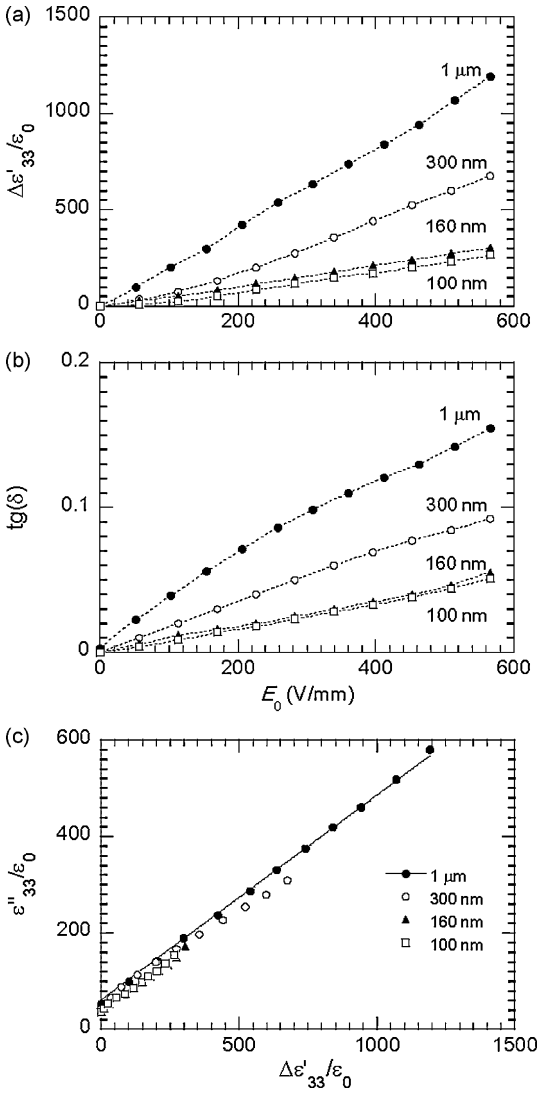

Fig. 6. ac electric field dependences of the dielectric constant increment $\Delta\varepsilon'$ (a), dielectric losses at 1 kHz (b), and the ratio between the dielectric losses ε'' and $\Delta\varepsilon'$ (c) for PIN–37PT poled micro and nanostructured ceramics. The solid line in (c) corresponds to a fit with a slope equal to 0.42. See Table 1 for m_ε ratios.

tructured ceramics, the better is the stability under high electric field.

In order to check first the validity of the Rayleigh model, the dielectric response of nanostructured ceramics was analyzed. In this model the real and imaginary dielectric constants, ε' and ε'', can be expressed in the form[12–14]:

$$\varepsilon' = \varepsilon_L + \alpha E_0$$

$$\varepsilon'' = \frac{4}{3\pi}\alpha E_0$$

where E_0 is the amplitude of the applied ac electric field. The ratio between the increase of the imaginary dielectric constant and the increase of the real dielectric constant is a constant that does not depend on the material:

$$m_\varepsilon = \frac{\Delta\varepsilon''}{\Delta\varepsilon'} = \frac{4}{3\pi} \cong 0.42$$

Fig. 6c shows that the slopes of the curves $\varepsilon'' = f(\Delta\varepsilon')$ are very close to this value predicted by the Rayleigh model. These results as well as the linear dependence of the increase of dielectric constant versus the electric field amplitude show that the Rayleigh law is confirmed for each nanostructured ceramic. Table 1 shows the ratios m_ε values as well as Rayleigh coefficient α of PIN–37PT nanostructured ceramics. The coefficient α decreases when the grain size decreases down to ~100 nm: the Rayleigh coefficient is equal to 2.1×10^{-3} and 4.9×10^{-4} m/V for 1 μm and 100 nm, respectively. This behavior can be explained on the basis of the effect of internal stresses originating in the poled ceramic[9,15] and by an increase of the surface to volume of domains ratio when the grain size is reduced, for grain sizes bigger than 1–3 μm; but this domain wall contribution decreases for grain sizes lower than 1 μm. It was shown in $BaTiO_3$ that grains are essentially single domain when their size is reduced below 500–300 nm,[16–18] and the extrinsic effect could disappear. Reduction of grain size leads so to a reduction of the density and the size of domain walls as well as its mobility. Even if domains include several grains,[19] the grain boundary

could limit the domain wall mobility and reduce the extrinsic effect. Since non-linearity is related to irreversible motion of domain walls under high electric field, reduction of grain size leads to a decrease of the Rayleigh coefficient. Thus, the decrease of extrinsic effects due to the decrease of grain size, results in a decrease of the non-linear behavior allowing a better adaptation of these nanostructured ceramics to power devices.

4. Conclusions

$0.63Pb(In_{1/2}Nb_{1/2})–0.37PbTiO_3$ nanopowders have been successfully synthesized by attrition milling followed by a high-energy ball milling process. On average, 8–10 h high-energy ball milling was necessary to obtain nanopowders with grain size in the 20–30 nm range. These powders can be directly used to prepare PIN–37PT nanostructured ceramics. Nanoceramics exhibiting relative density of 98% were sintered by hot pressing. Relatively homogeneous nanostructures of dense ceramics were observed. The dielectric and piezoelectric properties of the PIN–37PT nanoceramics remain almost constant when the grain size decreases down to 160 nm. These PIN–PT nanostructured ceramics present a better stability under high ac electric field; the lower is the grain size the higher is the stability. This result is attractive for the acoustics transducers applications. Moreover, the behavior of 100 nm grain sized dense ceramics is not consistent with the evolution of properties versus grain size. The electromechanical properties obtained on 100 nm nanostructured ceramics were much lower than on 160 nm nanostructured ceramic. This could be caused by a reduction of ferroelectricity probably due to a size-induced polarization rotation,[8] for grain sizes under 160 nm. Future work is needed in order to explain this behavior, in particular the challenge concerning nanostructured ceramics with the grain size under 100 nm.

Acknowledgments

H. Dammak gratefully acknowledge helpful discussions with P. Vajda.

References

1. Alberta EF, Bhalla AS. Piezoelectric properties of PIN–PT solid solution ceramics. *J Korean Phys Soc* 1998;**32**:S1265–7.
2. Alberta EF, Bhalla AS. Low-temperature property investigation of the lead indium–niobate–lead nickel–niobate solid solution. *J Phys Chem Sol* 2002;**63**:1759–69.
3. Augier C, PhamThi M, Dammak H, Gaucher P. Fine grains ceramics of PIN–PT, PIN–PMN–PT and PMN–PT systems: drift of the dielectric constant under high electric field. *Ultrasonics* 2006;**44**:E627–31.
4. Augier C, PhamThi M, Dammak H, Gaucher P. Phase diagram of high T_C PIN–PT ceramics. *J Eur Ceram Soc* 2005;**25**:2429–32.
5. Kong LB, Zhu W, Tan OK. Preparation and characterization of $Pb(Zr_{0.52}Ti_{0.48})O_3$ ceramics from high-energy ball milling powders. *Mater Lett* 2000;**42**:232–9.
6. Berar JF.*IUCr: Sat. meeting on powder diffractometry*. 1990.
7. Ménoret C, Kiat J-M, Dkhil B, Dunlop M, Dammak H, Hernandez O. Structural evolution and polar order in $Sr_{1-x}Ba_xTiO_3$. *Phys Rev B* 2002;**65**:224104.
8. Carreaud J, Kiat JM, Dkhil B, Alguero M, Ricote J, Jimenez R, Holc J, Kosec M. Monoclinic morphotropic phase and grain size-induced polarization rotation in $PbMg_{1/3}Nb_{2/3}O_3$-$PbTiO_3$. *Appl Phys Lett* 2006;**89**:252906.
9. Zhao Z, Buscaglia V, Viviani M, Buscaglia MT, Mitoseriu L, Testino A, Nygren M, Johnson M, Nanni P. Grain-size effects on the ferroelectric behavior of dense nanocrystalline $BaTiO_3$ ceramics. *Phys Rev B* 2004;**70**:024107.
10. Zhang XL. Dielectric and piezoelectric properties of modified lead titanate zirconate ceramics from 4.2 to 300 K. *J Mater Sci* 1983;**18**:968–72.
11. Damjanovic D. Stress and frequency dependence of the direct piezoelectric effect in ferroelectric ceramics. *J Appl Phys* 1997;**82**:1788–97.
12. Damjanovic D, Demartin M. Contribution of the irreversible displacement of domain walls to the piezoelectric effect in barium titanate and lead zirconate titanate ceramics. *J Phys Condens Matter* 1997;**9**:4943–53.
13. Garcia JE, Pérez R, Albareda A, Eiras JA. Non-linear dielectric and piezoelectric response in undoped and Nb^{5+} or Fe^{3+} doped PZT ceramic system. *J Eur Ceram Soc* 2007;**27**:4029–32.
14. Garcia JE, Perez R, Albareda A. Contribution of reversible processes to the non-linear dielectric response in hard lead zirconate titanate ceramics. *J Phys: Condens Matter* 2005;**17**:7143–50.
15. Garcia JE, Perez R, Ochoa DA, Albareda A, Lente MH, Eiras JA. Evaluation of domain wall motion in lead zirconate titanate ceramics by non linear response measurements. *J Appl Phys* 2008;**103**:054108.
16. Sarrazin P, Thierry B, Niepce JC. Forming pressure-dependence of the ferroelectric domain-structure in green barium-titanate pellets. *J Eur Ceram Soc* 1995;**15**:623–9.
17. Frey MH, Xu Z, Han P, Payne DA. The role of interfaces on an apparent grain size effect on the dielectric properties for ferroelectric barium titanate ceramics. *Ferroelectrics* 1998;**206**:337–53.
18. Arlt G, Hennings D, de With G. Dielectric-properties of fine-grained barium-titanate ceramics. *J Appl Phys* 1985;**58**:1619–25.
19. Buscaglia MT, Viviani M, Buscaglia V, Mitoseriu L, Testino A, Nanni P, Zhao Z, Nygren M, Harnagea C, Piazza D, Galassi C. High Dielectric constant and frozen macroscopic polarization in dense nanocrystalline $BaTiO_3$ ceramics. *Phys Rev B* 2006;**73**:064114.